

# METHOD FOR CORRECTION OF THE SYSTEMATIC ERRORS IN DETECTED SHOCK WAVE PASSAGE TIMES IN THE SHOCK TUBE

Francisco Javier Hernández Castro<sup>1</sup>, Andrej Svete<sup>2</sup>, Jože Kutin<sup>3</sup>

Laboratory of Measurements in Process Engineering, Faculty of Mechanical Engineering, University of Ljubljana, Slovenia, <sup>1</sup>[javier.hernandez-castro@fs.uni-lj.si](mailto:javier.hernandez-castro@fs.uni-lj.si), <sup>2</sup>[andrej.svete@fs.uni-lj.si](mailto:andrej.svete@fs.uni-lj.si), <sup>3</sup>[joze.kutin@fs.uni-lj.si](mailto:joze.kutin@fs.uni-lj.si)

## Abstract:

The most important uncertainty component of the pressure step signal determined at the end-wall of the shock tube is associated with the uncertainties of the shock wave velocity and the arrival time of the shock front. Both are determined using a time-of-flight method and are therefore greatly affected by the errors in the detected times of the shock wave passages over the side-wall pressure sensors installed along the shock tube. This paper introduces a method for an automated correction of the systematic errors due to non-ideal dynamic response of the side-wall pressure sensors.

**Keywords:** diaphragmless shock tube; time-varying pressure; time-of-flight method; dynamic response; correction

## 1. INTRODUCTION

The need for more accurate dynamic measurements of pressure has been driven by the advances in aerospace engineering, internal combustion engines and other industrial applications [1]. In recent years, shock tubes have been thoroughly studied as aperiodic pressure generators capable of acting as a primary standard for dynamic calibration of pressure sensors because they are capable of generating almost ideal and metrologically traceable pressure steps.

In the shock tube, shock waves are generated by the sudden opening of the connection between the high-pressure (driver) section and the low-pressure (driven) section. The shock wave propagates into the latter until reaching the end-wall, where the pressure sensor to be calibrated is placed. Studies have shown that the end-wall shock wave velocity, which is measured using a time-of-flight (TOF) method, is the major contributor to the uncertainty in the amplitude of the determined end-wall pressure step [2]-[5]. The uncertainties of the end-wall shock wave velocity  $V_{\text{wall}}$  and the arrival time of the shock front at the end-wall  $t_{\text{wall}}$  include also the uncertainties of the detected times of the shock wave passages over the locations of the side-wall sensors. In this work a method for correction of the

systematic errors in the passage times of the shock waves due to non-ideal dynamic response of the side-wall pressure sensors is presented.

## 2. PROBLEM BACKGROUND

The dynamic response of the side-wall pressure measurement system (PMS) used for determining the shock wave passages depends on its frequency response function (FRF), the velocity of the shock wave at the locations of the side-wall pressure sensors  $V_i$  and the effective diameter of the side-wall pressure sensors  $D$ . In the recent work [6], we have developed the physical mathematical model that simulates the side-wall PMS input and output signals. The developed model considers the integral effect of the shock wave pressure on the pressure sensor diaphragm's effective area covered by the shock wave and determines the response of the PMS to the input pressure by considering the FRF of the complete side-wall PMS chain. The use of the physical model requires the information about  $V_i$  and  $D$ . The effective diameter of four identical side-wall pressure sensors installed along the developed diaphragmless shock tube was determined based on the best fit between the normalised measured output signals of the side-wall PMS and the theoretical output signals obtained with the physical model [6].

The errors in the detection of the shock front passage times were furthermore determined as the differences between the detected passage times determined by applying the mean-shift-based (MSB) method to the simulated output signals of the side-wall PMS and the passage times of the shock wave over the centres of the side-wall pressure sensors determined as time at which the normalised simulated input signals reach the value of 0.5, see Figure 1. The values for these errors ranged between  $1.271 \cdot 10^{-3}$  ms and  $1.285 \cdot 10^{-3}$  ms for the lowest shock wave velocities measured at the location of the last pressure sensor installed downstream of the driven section  $x_4$  and highest measured shock wave velocities at the location of the first sensor  $x_1$ , respectively.

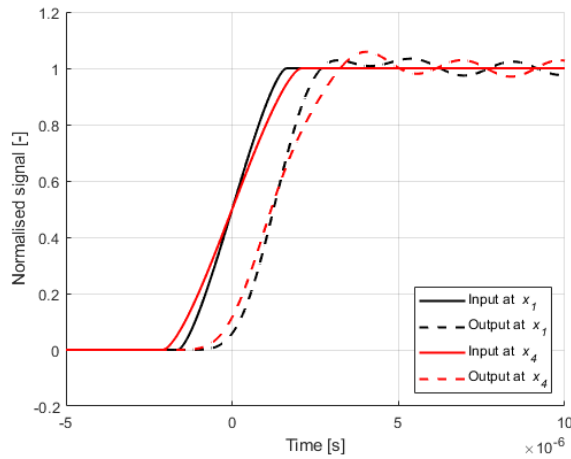


Figure 1: Simulated input and output signals for the maximum (black) and minimum (red) measured shock wave velocities and an effective sensor diameter of 2.6 mm

Finally, the errors in the amplitude and the initial time of the pressure step due to the errors in the detection of the shock front passage times were evaluated in accordance to JCGM 100:2008 [7]. The results showed that the relative errors in the pressure step amplitudes are less than 0.0003% and can be therefore considered negligible in comparison to the target amplitude measurement uncertainty in dynamic calibrations of pressure sensors. The errors in the initial time of the pressure step were similar to those of the last side-wall pressure sensor and are up to  $1.278 \cdot 10^{-3}$  ms. This error might seem small, but it represents significant systematic error in the determination of the phase frequency characteristics of the pressure sensors using a shock tube, e.g., up to  $46^\circ$  at the frequency of 100 kHz.

### 3. METHOD FOR CORRECTION OF THE SYSTEMATIC ERRORS

Based on the recent findings, we implemented an automated correction for the systematic errors in the detection of the shock front passage times over the side-wall pressure sensors. The program, which was realized in MATLAB, takes as an input the PMS voltage output signal  $U(t)$  and, with the corrected passage times, determines the reference pressure step signal at the end-wall of the driven section of the shock tube. The operation of the program is schematically presented in Figure 2 and detailed afterwards. With the use of the measured input the program calculates the shock wave passage times by applying the MSB method. Those times are used to calculate an approximation of the shock wave velocity along the shock-tube from which it extracts the velocity at the locations of the side-wall sensors. Using the determined shock wave velocities as well as the FRF and the effective diameter  $D$  of the side-wall pressure sensors, the simulated input and output signals of the PMS are

calculated. The errors in the shock wave passage are determined from the differences between such input and output signals. Finally, the passage times corrected for the determined systematic errors are used to determine the amplitude and the initial time of the end-wall pressure signal.

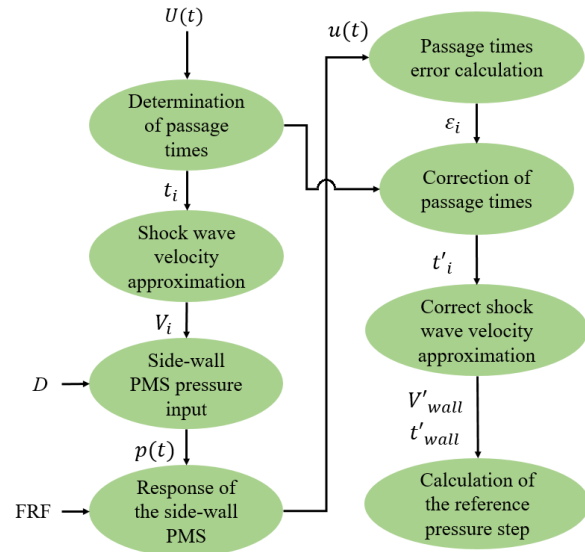


Figure 2: Flowchart presenting the program for correcting the errors associated with the shock wave passage times over the side-wall pressure sensors

#### Determination of the passage times:

The shock wave passage times over the centre of the diaphragm of the side-wall pressure sensors  $t_i$  are determined by the times of the local maximum gradients in  $U(t)$  which are found by transformation using the MSB method. Such method calculates the differences between the sum of the adjacent signal segments of the same width that are shifted in time with respect to each other by the width of one segment. The MSB method is described by:

$$U_{\text{MSB}}(nT_s + WT_s) = \sum_n^{n+W} U(nT_s + WT_s) - \sum_n^{n+W} U(nT_s), \quad (1)$$

where  $T_s$  is the sampling period,  $W = 50$  is the number of samples of the signal segments and  $n = [0, 1 \dots N - 1 - 2W]$ , where  $N$  is the total number of samples in  $U(t)$ .

#### Shock wave velocity approximation:

The variation of the shock wave velocity along the tube is considered to follow a quadratic model in the form  $V(x) = ax^2 + bx + c$ . To obtain the coefficients  $a$ ,  $b$  and  $c$  it is necessary to solve the system of three equations:

$$t_{i+1} - t_i = \int_{x_i}^{x_{i+1}} \frac{dx}{V(x)}, \quad (2)$$

where  $i = 1, 2, 3$ .

### Side-wall PMS pressure input:

The pressure input signal normalised between 0 and 1 is defined by the relative portion of the sensor diaphragm's effective area affected by the shock wave passage. If we assume the circular sensor's diaphragm with the effective diameter  $D$  that has the same sensitivity at all points and the wave velocity  $V_i$ , the pressure input is:

$$p(t) = \begin{cases} 0, & x_{\text{rel}}(t) \leq 0 \\ A_{\text{rel}}(t), & 0 < x_{\text{rel}}(t) < 1, \\ 1, & x_{\text{rel}}(t) \geq 1 \end{cases} \quad (3)$$

where  $x_{\text{rel}}(t) = V_i \cdot t/D$  and the relative portion of the diaphragm excited by the shock wave passage is:

$$A_{\text{rel}}(t) = \frac{\theta(t) - \sin\theta(t)}{2\pi}, \quad (4)$$

where  $\theta(t)$  is the central angle in radians:

$$\theta(t) = 2 \arccos(1 - 2 x_{\text{rel}}(t)). \quad (5)$$

### Response of the side-wall PMS:

The normalised PMS voltage output signal can be determined the Fourier transform method as:

$$u(t) = \mathfrak{F}^{-1}(\mathfrak{F}(p^*(t))H_{\text{PMS}}(\omega)), \quad (6)$$

where  $p^*(t)$  is the converted normalised pressure input signal using the Gans-Nahman technique [8]:

$$p^*(t) = \begin{cases} p(t), & 0 \leq t \leq T \\ 1 - p(t - T), & T < t \leq 2T \end{cases} \quad (7)$$

which satisfies  $p^*(0) = p^*(2T) = 0$  and the FRF of the complete side-wall PMS  $H_{\text{PMS}}(\omega)$  is the product of the FRFs of the pressure sensor  $H_S(\omega)$ , the charge amplifier  $H_{\text{ca}}(\omega)$  and the digitizer  $H_{\text{dig}}(\omega)$ . The FRF of the pressure sensor, which is modelled as the second-order dynamic system, is:

$$H_S(\omega) = \frac{1}{1 - \frac{\omega^2}{\omega_n^2} + 2i\xi\frac{\omega}{\omega_n}}, \quad (8)$$

where  $f_n = \omega_n/(2\pi) = 341.5$  kHz is the undamped natural frequency and  $\xi = 0.0047$  is the damping ratio; both were estimated in [5]. The FRF of the charge amplifier is [9]:

$$H_{\text{ca}}(\omega) = \frac{1}{1 - \frac{\omega^2}{\omega_{\text{c,ca}}^2} + 1.4142i\frac{\omega}{\omega_{\text{c,ca}}}}, \quad (9)$$

where  $f_{\text{c,ca}} = \omega_{\text{c,ca}}/(2\pi) = 200$  kHz is the cut-off frequency of the charge amplifier. The FRF of the digitizer is [9]:

$$H_{\text{dig}}(\omega) = \frac{1}{\prod_i^3 \left( 1 - b_i \frac{\omega^2}{\omega_{\text{c,dig}}^2} + a_i i \frac{\omega}{\omega_{\text{c,dig}}} \right)}, \quad (10)$$

where  $a_1 = 1.2217$ ,  $a_2 = 0.9686$ ,  $a_3 = 0.5131$ ,  $b_1 = 0.3887$ ,  $b_2 = 0.3505$ ,  $b_3 = 0.2756$  and  $f_{\text{c,dig}} = \omega_{\text{c,dig}}/(2\pi) = 13.9$  MHz is the cut-off frequency of the digitizer.

### Passage times error calculation:

By applying the MSB method to the simulated input and output signals of each side-wall PMS, it is possible to calculate the systematic errors in the detection of the shock wave passage as difference between the time of the shock wave passage and the time of detection, as shown in Figure 3.

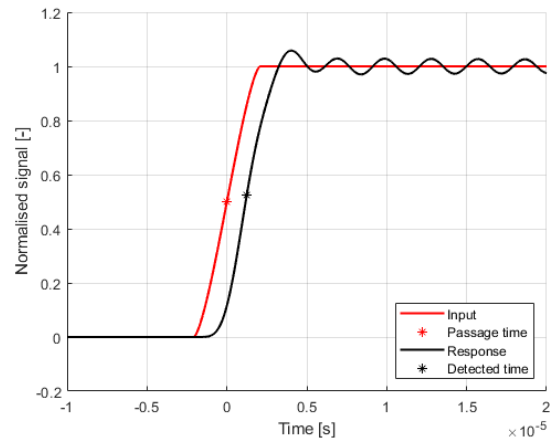


Figure 3: Input and output signals with the respective shock wave passage time over the last side-wall pressure sensor and its detected time at the lowest initial driven pressure

### Correction of passage times and the correct shock wave velocity approximation:

The systematic errors in the detection of the shock wave passage  $\varepsilon_i$  are applied to the passage times in order to obtain the corrected passage times  $t'_i$  as:

$$t'_i = t_i - \varepsilon_i, \quad (11)$$

and are substituted into equation (2) to obtain the corrected shock wave velocity  $V'(x)$ .

### Calculation of the reference pressure step:

Finally, the amplitude of the reference pressure step is calculated as:

$$\Delta P = 2 P_1 \frac{\gamma}{\gamma^2 - 1} (M_{\text{wall}}^2 - 1) \cdot \left( \frac{M_{\text{wall}}^2 (3\gamma - 1) + 3 - \gamma}{M_{\text{wall}}^2 + \frac{2}{\gamma - 1}} \right), \quad (12)$$

where  $p_1$  is the initial absolute pressure of the gas in the driven section,  $\gamma$  is the adiabatic index,  $M_{\text{wall}} =$

$V'_{\text{wall}}/a_1$  is the shock wave Mach number at the end-wall,  $a_1 = \sqrt{\gamma R T_1}$  is the speed of sound and  $R$  is the specific gas constant. The arrival time of the shock front at the end-wall  $t'_{\text{wall}}$  is calculated as:

$$t'_{\text{wall}} = t'_4 + \int_{x_4}^{x_{\text{wall}}} \frac{dx}{V'(x)}, \quad (13)$$

where  $x_{\text{wall}}$  is the location of the end-wall.

#### 4. RESULTS

Figure 4 and Figure 5 present the results obtained by applying the proposed method to the results of two measurements at different initial driver pressures, i.e., 4 and 10 MPa, respectively. Before applying the correction, the time of arrival of the shock front gave unphysical results as the measured pressure signal started to rise before the reference pressure step.

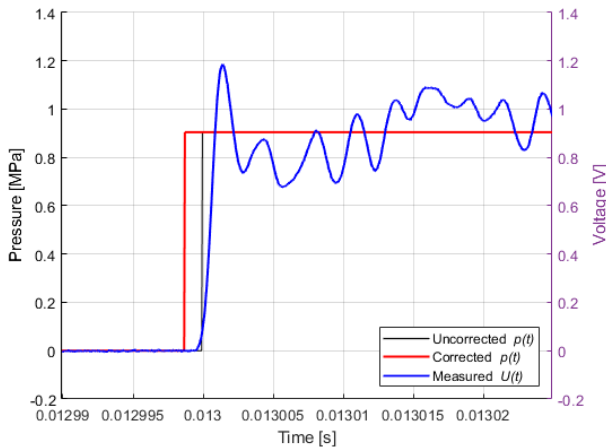


Figure 4: End-wall PMS output voltage and reference end-wall pressure step before and after implementing the correction; at initial driver pressure of 4 MPa

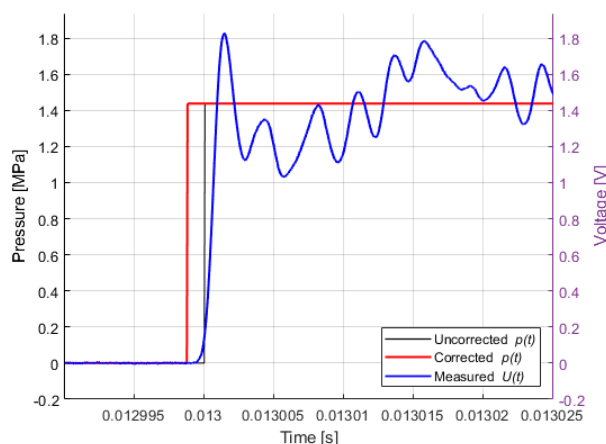


Figure 5: End-wall PMS output voltage and reference end-wall pressure step before and after implementing the correction; at initial driver pressure of 10 MPa

Both figures show that, after the correction, this anomaly is eliminated. Instead, the new time of arrival and the response of the sensor are consistent with each other. The fact that the time of the

response of the PMS lags behind  $t'_{\text{wall}}$  is expected due to the internal dynamics of the PMS. In terms of the amplitude of the reference pressure step, the results show that the relative change is in the order of only 0.0003 % and therefore is not evident in the figures.

#### 5. CONCLUSIONS

We proposed and automatized a method for the correction of the systematic errors induced by non-ideal dynamic measurements of the shock wave passage by the side-wall PMS. The method calculates the shock wave passage times over the centres of the diaphragms of the side-wall pressure sensors which are later used to calculate the shock wave velocity based on a quadratic extrapolation model. The shock wave velocity at the position of the sensors is then used to simulate the PMS response to the pressure input. The systematic error in the detection of the shock wave passage times over the centres of the side-wall pressure sensors, which is defined as the difference between the time of the shock wave passage and the time of detection, is then used for correcting the originally calculated shock wave passage times. Then, the corrected shock wave passage times are used to obtain the corrected shock wave velocity at the end wall, which is used to calculate the corrected amplitude and time of arrival of the reference pressure step at the end-wall of the driven section of the shock tube. Before the correction, the response of the PMS was prior to the time of arrival of the shock wave at the end-wall, which is physically incorrect. After the correction, the response of the PMS shows some lag behind the arrival of the shock wave at the end-wall, which is logical in a view of the internal dynamics of the PMS and proves the successful implementation of the correction.

#### ACKNOWLEDGEMENTS

The authors acknowledge the financial support of the Slovenian Research Agency for the project Advanced shock tube system for high-frequency primary dynamic pressure calibration (project No. J2-3054), in addition to the research core funding (No. P2-0223).

#### REFERENCES

- [1] J. Hjelmgren, Dynamic Measurement of Pressure - A Literature Survey, SP Swedish National Testing and Research Institute, 2002.
- [2] S. Downes, A. Knott and I. Robinson, "Uncertainty estimation of shock tube pressure steps", in Proc. of 21st IMEKO World Congress, Prague, Czechia, 2015, pp. 1648-1651. Online [Accessed 20230102]: <https://www.imeko.org/publications/wc-2015/IMEKO-WC-2015-TC16-336.pdf>

- [3] A. Knott, I. A. Robinson, “Dynamic Characterisation of Pressure Transducers Using Shock Tube Methods”, *Trans. Inst. Meas. Control*, vol. 42, 2019, no. 4, pp. 743-748.  
DOI: [10.1088/1742-6596/1065/16/162002](https://doi.org/10.1088/1742-6596/1065/16/162002)
- [4] A. Svete, J. Kutin, “Characterization of A Newly Developed Diaphragmless Shock Tube for The Primary Dynamic Calibration of Pressure Meters”, *Metrologia*, vol. 57, 2020, no. 5, 055009.  
DOI: [10.1088/1681-7575/ab8f79](https://doi.org/10.1088/1681-7575/ab8f79)
- [5] A. Svete, J. Kutin, “Identifying The High-Frequency Response of a Piezoelectric Pressure Measurement System Using a Shock Tube Primary Method”, *Mech. Syst. Signal Process*, vol. 162, 2021, 108014.  
DOI: [10.1016/j.ymssp.2021.108014](https://doi.org/10.1016/j.ymssp.2021.108014)
- [6] A. Svete, F. J. Hernández Castro, J. Kutin, “Effect of the Dynamic Response of a Side-Wall Pressure Measurement System on Determining the Pressure Step Signal in a Shock Tube Using a Time-of-Flight Method”, *Sensors*, vol. 22, 2022, 2103.  
DOI: [10.3390/s22062103](https://doi.org/10.3390/s22062103)
- [7] BIPM, IEC, IFCC, ILAC, ISO; IUPAC; IUPAP; OIML, “Evaluation of Measurement Data—Guide to the Expression of Uncertainty in Measurement”; Tech Rep. JCGM 100: 2008; Joint Committee for Guides in Metrology: Paris, France, 2008.
- [8] W. L. Gans, N. S. Nahman, “Continuous and Discrete Fourier Transforms of Steplike Waveforms”, *IEEE Trans. Instrum. Meas.*, no. 2, 1982, pp. 97–101.  
DOI: [10.1109/TIM.1982.6312529](https://doi.org/10.1109/TIM.1982.6312529)
- [9] R. Mancini. “Op Amps for Everyone”, Texas Instruments, 2002.